Vertical Dimension of Hydrated Biological Samples in Tapping Mode Scanning Force Microscopy

Frank A. Schabert and Jürgen P. Rabe
Humboldt University of Berlin, Department of Physics, D-10115 Berlin, Germany

ABSTRACT The vertical dimensions of the well-characterized test samples tobacco mosaic virus, T4 bacteriophage polyhead, purple membrane, and hexagonally packed intermediate (HPI) layer were investigated by tapping mode scanning force microscopy (SFM) in solution. Purple membrane and HPI layer were imaged in both contact mode and tapping mode SFM for direct comparison. All vertical dimensions match the known heights. The practical implications of the absence of frictional forces in tapping mode are discussed.

INTRODUCTION

Thirteen years after the invention of the STM (Binnig and Rohrer, 1982) and nine years after the development of the scanning force microscope (SFM) (Binnig et al., 1986), the biological application of scanning probe microscopy (SPM) is still limited to a small community (Hansma and Hoh, 1994). The outstanding resolution of the SFM, most notably if operated in the attractive regime in aqueous solution (Ohnesorge and Binnig, 1993), has fostered the hope that the SFM might develop into an elegant and easy-to-use microscope for the investigation of biological specimens.

In the conventional repulsive force contact mode SFM frictional forces require an efficient immobilization of the biological specimen on a flat substrate (Engel, 1991). For isolated biological macromolecules covalent linking was found to be helpful (Hegner et al., 1993; Karrasch et al., 1993). Membrane proteins in 2D crystalline arrays (Butt et al., 1990; Hoh et al., 1991; Yang et al., 1993; Schabert and Engel, 1994; Müller et al., 1995b) or huge macromolecular assemblies (Goldie et al., 1994) can be reasonably stable against displacements by the tip when adsorbed to a solid substrate by electrostatic interaction. Tapping mode operation of the SFM in air (Elings and Kjoller, 1992; Elings and Gurley, 1993) does circumvent the large frictional forces present in contact mode. Highly promising results were also obtained with tapping mode operation in aqueous solution (Bezanilla et al., 1994; Hansma et al., 1994; Radmacher et al., 1994); however, dramatically nonreproducible specimen heights were reported (Radmacher et al., 1994, and personal communication). The present work demonstrates that reliable height data can be obtained by tapping mode SFM in solution for various biological macromolecular assemblies, using an oscillating fluid cell and tapping frequencies around or below 10 kHz.

Received for publication 10 October 1995 and in final form 14 December 1995.

Address reprint requests to Dr. Frank Schabert, Humboldt-University of Berlin, Departmant of Physics, Invalidenstrasse 110, D-10115 Berlin, Germany. Tel.: +49-30-2803-419; Fax: +49-30-2803-232; E-mail: schabert@physik.hu-berlin.de.

© 1996 by the Biophysical Society

0006-3495/96/03/1514/07 $2.00

MATERIALS AND METHODS

Materials

Tobacco mosaic virus (TMV) was produced by Dr. Jean Witz (Institut de Biologie Moleculaire et Cellulaire, Strasbourg, France). A-type polyheads were prepared as described (Steven et al., 1976). Mutants (20^-) of T4 bacteriophages were propagated and titrated on the permissive host *Escherichia coli* CR 63. *E. coli* B^e was used as a nonpermissive host. Purple membranes of *Halobacterium salinarium* strain ET1001 were isolated as described (Oesterheld and Stoeckenius, 1974). The membranes were kept at 4°C before adsorption to mica at room temperature. The hexagonally packed intermediate (HPI) layer of *Deinococcus radiodurans* was purified at the Max Planck Institute for Biochemistry (Martinsried, Germany) (Baumeister et al., 1986).

Sample preparation

Mica sheets were stamped into round pieces of 5 mm diameter using a punch and die set to maintain nicely cleavable edges. Mica discs were glued onto 10-mm-diameter teflon supports that were mounted on a magnetic steel disc that served as a sample holder for the SFM. Similarly, a 12 $\times$ 12 mm^2 square of highly oriented pyrolytic graphite (HOPG) (grade ZYH; Advanced Ceramics, Cleveland, OH) was glued to a magnetic sample holder. Two microliters of sample solution (between 0.1 and 1 mg/ml) was applied to the freshly cleaved mica or HOPG for 3 min and then washed several times with buffer solution.

Instrumentation

A commercial SFM (Nanoscope III; Digital Instruments, Santa Barbara, CA) equipped with either a 13-μm scanner (E-scanner) or a 160-μm scanner (J-scanner) was placed on a granite slab. The microscope stage was hanging from soft bunjee cords with a single point attachment. The resonance frequency of this suspension was slightly below 0.5 Hz (for both the vertical and the pendulum oscillation modes). For tapping mode SFM in solution a new commercial tapping mode fluid cell (Digital Instruments) was used without the O-ring. Instead a latex barrier was placed over the piezo scanner. Si_3N_4 cantilevers with 100-μm-long and 15-μm-wide V-shaped legs from two sources (Digital Instruments and Olympus Optical Co., Scientific Equipment Division, Japan) with different tip geometries (oxide sharpened pyramid, oriented twin peaks and conventional pyramid) were used. Tapping in solution was performed by oscillating the entire glass fluid cell via a piezoelectric actuator. Resonance peaks in the fre-

quency response of the cantilever were chosen for the tapping mode oscillation. The quality of the resonance peak was significantly lower than in air, and multiple peaks frequently appeared. Generally the lowest frequency was chosen for operation. The typical tapping frequency was 9 kHz. Changing from contact mode into tapping mode operation was easily performed by withdrawing the tip and setting a switch. Thus the cantilevers' position on the sample was maintained.

Operation of the SFM

Contact mode SFM started with carefully taking force curves to calibrate the deflection of the cantilever with respect to the vertical position of the sample. Imaging was performed in the error-signal mode (Putman et al., 1992) at an angle of 90° with respect to the long axis of the cantilever. The deflection signal obtained in the trace and the height signal in the retrace direction were simultaneously recorded. Feedback parameters were optimized by reducing the deflection and therefore increasing the height signal at minimum force. For high resolution and critical evaluation of the vertical dimension the height was recorded in the trace and retrace directions. The scan speed was chosen depending on the scan size. A typical line frequency was 3 Hz, i.e., three lines backward and forward were recorded per second. Vertical thermal drift of the cantilever deflection was measured to be approximately 1 nm/min.

Tapping mode SFM was performed similarly to contact mode. The amplitude of the oscillation was carefully calibrated with respect to the vertical position of the scanner. Imaging was performed displaying the amplitude signal (incoming signal for the feedback system) of the cantilever in the trace and the height signal (output of the feedback system) in the retrace direction. Feedback parameters were obtained by minimizing changes of the amplitude signal. The amplitude signal is unaffected by the thermal drift of the cantilever. The damping of the cantilever was set to 1 to 3 nm, corresponding to a force of 100 to 300 pN for every tap on the sample (assuming no resonance). The oscillation amplitude of the tip was typically set to 20 nm. The force between tip and sample was constant within an hour. The scan speed was proportional to the scan size, and the corresponding line frequency was 1.5 Hz (three lines back and forward were recorded every 2 s). The vertical translation of the scanner was calibrated using monatomic steps on graphite (E-scanner) or 180-nm-deep structures on a reference sample (J-scanner) provided by Digital Instruments.

Data analysis

The vertical dimension of the biomolecules was determined from individual height profiles using the data analysis facilities of the Nanoscope software. The average and the standard deviation were calculated independently. The number of analyzed height profiles N varied between 200 and 613. The sample tilt was removed by subtracting a plane that was manually fitted to the substrate of the sample. Nevertheless, small tilt angles of the substrates sometimes still remained. In those cases (especially for the rodlike objects) the height was measured against and with the slope. Although the average height is not affected, the standard deviation is slightly increased. All tapping mode heights were acquired by using two or more different cantilevers.

RESULTS

In tapping mode SFM the amplitude of the cantilever oscillation remained practically constant for hours, whereas in contact mode the cantilever deflection drifted even after hours of thermal relaxation at a rate of 1 nm/min. Therefore, in contact mode, manual correction of the set point during the experiment is necessary to maintain a constant force below 500 pN (Schabert and Engel, 1994). In tapping mode SFM, on the other hand, no correction of the set point amplitude is needed. Even shortly after changing the buffer or the cantilever, tapping mode SFM is not sensitive to the changes of the deflection angle of the cantilever. Therefore, tapping mode imaging is less demanding in terms of operator interaction.

Four biological samples were imaged by tapping mode SFM, i.e., two cylindrically shaped macromolecular assemblies and two membrane proteins in native 2D crystals. For direct comparison topographs of the membrane proteins were recorded in both tapping and contact mode operation. All samples are well characterized with respect to their morphologies and their molecular structures.

The first sample was TMV, which is often used as a test sample, because its structure is solved to atomic resolution by x-ray crystallography (Namba and Stubbs, 1986). SFM investigations of TMV have been carried out in air (Zenhausern et al., 1992; Frommer et al., 1993; Vesenka et al., 1993), but imaging in a native buffer solution has not yet been achieved, because contact mode SFM pushes the rodlike TMV aside (Fig. 1 *a*). Although involved surface chemistry was successfully used to unspecifically immobilize various proteins on glass coverslips, it surprisingly failed to immobilize TMV efficiently (Karrasch et al., 1993). Tapping mode SFM, however, enabled stable imaging of TMV (Fig. 1, *b* and *c*). No pushing aside of objects was observed, and successive scans did not reveal any degradation of the image quality. The height of the TMV rods in tapping mode was measured to be 18.2 nm ± 1 nm (N = 613). Unfortunately, tapping mode SFM did not resolve the fine structure of TMV; attempts to unveil the molecular stacks with a periodicity of 2.3 nm perpendicular to the axis of the rodlike virus were not successful (see Fig. 1 *c*).

The second object, the polyhead, is a hollow tubular structure folded from a hexagonal lattice ($a = b$ = 13 nm) of capsomers with a diameter of 50 to 65 nm. It varies in length from about one up to several micrometers. When adsorbed to a carbon film and dehydrated by freeze drying, polyheads collapse and form a 120-nm-wide band with 5-nm height (Amrein, 1989). Correspondingly, the wall thickness of these tubes is less then 3 nm. In contact mode SFM the polyhead did not collapse, provided fully hydrated structures were imaged in solution (Karrasch et al., 1993). However, successful imaging was found to be critically dependent on the feedback characteristics of the SFM (Schabert et al., 1994b). In the present work, tapping mode SFM enabled stable and reproducible imaging of polyheads (Fig. 2). The height of the polyheads was determined to be 54.6 nm ± 4.6 nm (N = 513). However, whereas individual capsomers of the polyheads were seen in contact mode SFM before (Karrasch et al., 1993), tapping mode SFM failed to reproduce this structure.

Our third sample was the purple membrane from *Halobacterium salinarium*. It is the first membrane protein that was imaged in solution at high resolution (Butt et al., 1990), but it required 5 years (Müller et al., 1995a,b) and highly optimized conditions (Engel et al.,

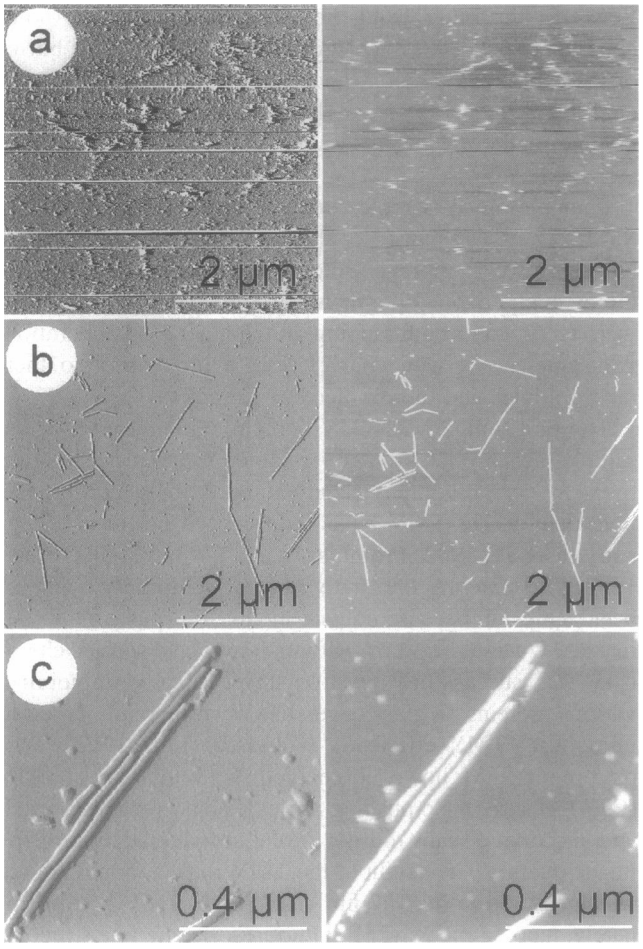

FIGURE 1 TMV on mica in solution. (*a*) In contact mode SFM the TMV rods were pushed aside. Horizontal lines are due to manual corrections of the set point, to maintain a minimum applied force of less than 300 pN. (*b*) In solution, tapping mode SFM with an amplitude of 196 nm (*b* and *c*) in 20 mM MES at pH 6 enables stable imaging. (*c*) Zooming (*b*) into higher magnification does not reveal any fine structure. All images were acquired in the error signal mode. The left column shows the input signal for the feedback (*a*, deflection; *b* and *c*, amplitude), whereas the right columns display the output of the feedback (*a*, *b*, and *c*, height signal). The gray scale corresponds to 1 nm (*a*) and 5 nm (*b* and *c*) for the left and 50 nm for the right column.

1995) before topographs were acquired that could be interpreted. A preparation protocol that enabled molecular resolution in contact mode SFM (data not shown; Müller et al., 1995b) was investigated with tapping mode SFM. Fig. 3 *a* shows several purple membrane patches adsorbed to mica. Background from the preparation and a few distorted scan lines can be seen. Most of the membranes exhibit a single layer thickness and fuzzy edges. The sample has been scanned several times to provide access to the flat monolayer surface. Shown in Fig. 3 *b* are purple membrane patches scanned in tapping mode. The edges of the purple membranes are less irregular than in contact mode. Most of the membranes reveal monolayer thickness and flat adsorption. Because of the lower

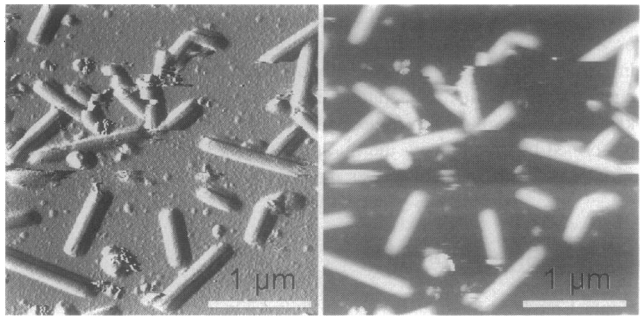

FIGURE 2 Polyheads on mica imaged in solution by tapping mode SFM. Tapping was performed with 150 nm amplitude in 200 mM Tris at pH 8. The left image shows the amplitude signal, whereas the right image represents the height (full gray scale corresponds to 1 nm for the amplitude and 100 nm for the height).

scan speed, the error signal of the feedback provides less contrast in tapping than in contact mode. A common problem in the preparation of two-dimensional structures is their undesired tendency to stack vertically. Although a monolayer of membrane patches is tightly adsorbed to the substrate, loosely adhered multilayers are also frequently observed. Only a few single monolayer membrane regions were found. Lower protein concentrations

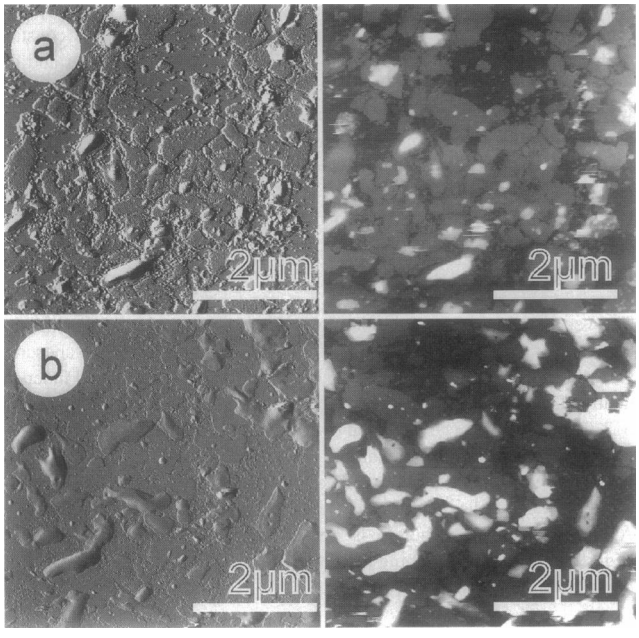

FIGURE 3 Purple membranes on mica imaged in solution. (*a*) In contact mode SFM several purple membrane patches can be seen to be adsorbed onto mica. The left image is the deflection signal recorded in the trace, whereas the height signal on the right was recorded in the retrace direction. (*b*) Tapped in 10 mM Tris, pH 8.2, the purple membranes appear similar to contact mode. Tapping was performed with 115 nm amplitude. The left image shows the amplitude in the trace, whereas the right image is the corresponding height signal recorded in the retrace direction. For the left column the gray scale corresponds to 5 nm, whereas the height data are shown with 30 nm (black to white) contrast.

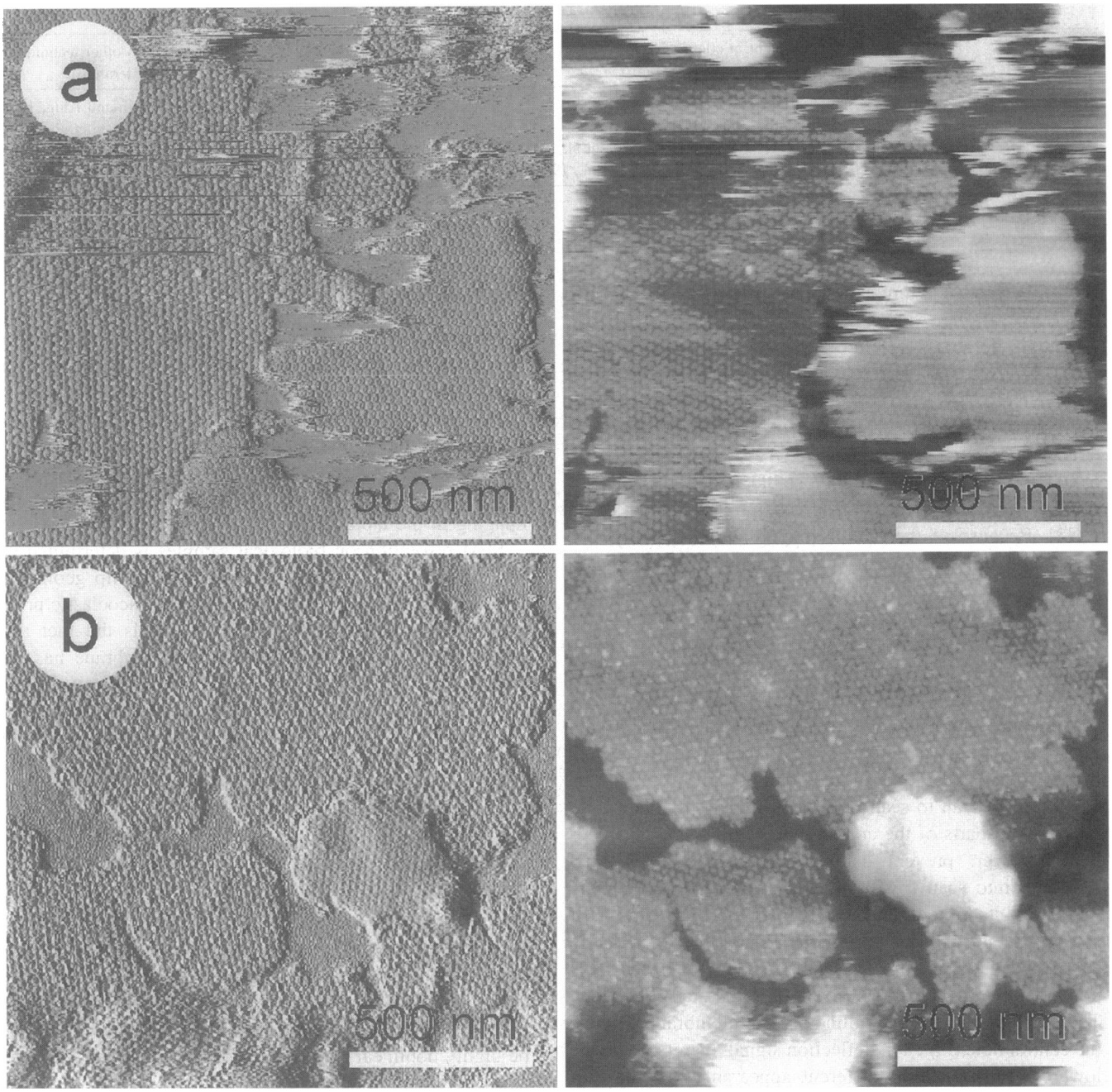

FIGURE 4 HPI layer adsorbed onto HOPG. (*a*) In contact mode the two sides of the HPI layer can be identified in different sheets. (*b*) In tapping mode the identical tip and sample barely identify both orientations. Tapping was performed in 20 mM MES, pH 6, with 19 nm amplitude. The images generated in the trace direction from the deflection (*a, left side*) and the amplitude (*b, left side*) signal have a vertical range of 1 nm. Both height data in the right column are shown with a gray scale corresponding to 20 nm.

resulted in incomplete coverage of the substrate rather than reduced stacking of the membranes. Repetitive scans in contact mode with a small increase in the applied force did remove most of the loosely bound material. In Fig. 3, *a* and *b*, stacking was not yet completely removed. Tapping and contact mode topographs have the same appearance (Fig. 3, *a* and *b*). Stacks of multiple layers (Fig. 3 *b*) are rounded in tapping mode and remain stable for several scans. Tapping mode required clearing the area on the sample by contact mode first. Pushing aside and deformation of samples were seen in tapping mode SFM when the scan speed was set too high. Nevertheless, a controlled dissection of membranes was not accomplished by raising scan speed and force as in contact mode (Hoh et al., 1991). The height of the purple membranes was measured to be 6.3 nm ± 0.4 nm (N = 468)

TABLE 1 Vertical dimension of biological macromolecules

	Height in contact mode (this work and literature)	Height in tapping mode (this work)	Height from other techniques (literature)
TMV		(18.2 ± 1) nm	18 nm (Unwin and Klug, 1974)
Polyheads	(57 ± 13) nm (Karrasch et al., 1993)	(54.6 ± 5) nm	50–60 nm (Steven et al., 1976)
HPI	(6.0 ± 0.7) nm, (6.6 ± 0.5) nm (Karrasch et al., 1993)	(6.0 ± 0.8) nm	
Purple membrane	(6.3 ± 0.4) nm, (5.6 ± 0.1) nm (Müller et al., 1995b)	(6.5 ± 0.5) nm	

in contact and 6.5 nm ± 0.5 nm (N = 251) in tapping mode operation.

Sample number 4 was the HPI layer from *Deinococcus radiodurans*, a popular test for scanning probe microscopy (Guckenberger et al., 1989; Wang et al., 1990; Amrein et al., 1991; Wiegräbe et al., 1991; Butt et al., 1992; Schabert et al., 1992, 1994b; Karrasch et al., 1993, 1994; Anselmetti et al., 1994). It is remarkably stable and withstands air drying with only little loss of its structure (Wildhaber et al., 1985). Because of the lateral support within 2D crystals, membrane proteins are sufficiently stable for imaging in contact mode SFM, even if each molecule is only slightly immobilized by the substrate. In contact mode (Fig. 4 *a*) the height of a protein layer was 6.0 nm ± 0.7 nm (N = 236), which matches 6.0 nm ± 0.8 nm (N = 200) for tapping mode SFM (Fig. 4 *b*). Whereas tapping mode SFM (Fig. 4 *b*) generates stable and reproducible images, the protein crystals were often damaged when scanning in contact mode (Fig. 4 *a*). Edges of membranes appear fuzzy and change from scan to scan (Fig. 4 *a*), indicating that the tip is removing parts of the crystal with every scan. This does not, however, prevent stable, high-resolution imaging. Zooming into scan frames, which are located completely within an intact membrane, easily enables the generation of several stable topographs without any visible degradation caused by the scan. In contact mode topographs the morphologies of the two sides of HPI are distinctly different. The outer side of the crystalline protein membrane exhibits the central hole (Fig. 4 *a*, deflection signal, membrane in the lower right part). Two different appearances of the HPI layer were also found in tapping mode, but a central hole is not visible on either side (Fig. 4 *b*). Tapping mode topographs reveal little information beyond the 18-nm lattice, whereas the identical tip and sample unveil more details in contact mode.

The vertical dimensions of all samples analyzed in this work are summarized and compared with references from the literature in Table 1. With the exception of the purple membrane, all tapping mode specimen heights match the reference experiments, and in the case of the purple membrane both our tapping and contact mode experiments show identical thickness. An artifact of the tapping process is therefore very unlikely. The accuracy of the height measurements seems higher than in contact mode for the polyheads, whereas it is smaller for the HPI layer.

DISCUSSION

A common feature of detection systems is that AC detection is more stable than DC techniques. More specifically, in tapping mode, SFM is insensitive to the actual position of the deflected beam on the split photodiode, because the amplitude of the oscillating deflection is detected. In contact mode, on the contrary, an offset is measured, which does drift thermally with time. The practical result is more stable imaging in the tapping mode.

SFM resolution on biological samples is determined by several factors, including the applied force, tip geometry, scan speed, and the frequency-dependent viscoelastic properties of the samples. Evidence for this is the fact that high-resolution imaging of the purple membrane has not only an upper but also as a lower scan speed limit (Müller et al., 1995b). Furthermore, Putman and co-workers demonstrated that mechanical properties of biological objects can differ significantly for DC contact mode and AC tapping mode detection (Putman, 1994; Putman et al., manuscript submitted for publication).

Previous tapping mode SFM experiments of biological objects resulted in false information on the vertical dimension (Hansma et al., 1994; Radmacher et al., 1994, and personal communication), whereas in the present work reliable height data were measured. It should be noted that most of the earlier tapping mode experiments were obtained by oscillating the scanner with common frequencies around 20 kHz. However, even small tube scanners are reported to be highly nonlinear at frequencies above 10 kHz (Stemmer and Engel, 1990), and phase shifts as well as higher oscillation modes occur. Our results indicate that lower frequencies and a scanner-independent oscillation of the fluid cell circumvent these difficulties.

Tapping mode SFM in solution has not yet shown high lateral resolution in the range from 5 nm down to the atomic scale. Fig. 4 suggests that the tip geometry is not responsible for the little detail that is visible in the tapping mode topographs, because upon switching the operation from tapping to contact mode the central hole of the HPI appears in the topograph. On the other hand, in tapping mode small differences are visible between different membranes, suggesting that the difference between the two sides of the HPI layer is detected. Our data suggest that the interaction between tip and sample in tapping mode SFM needs to be considered. In contact

mode the forces that enable stable high-resolution imaging on biological samples are known to be below 500 pN (Schabert and Engel, 1994; Engel et al., 1995; Müller et al., 1995a; Schabert and Engel, 1995; Schabert et al., 1995; Shao and Yang, 1995). The tapping mode SFM was operated at a set point, which corresponds typically to 2 nm damping of the amplitude. Given the nominal force constant of 0.1 N/m, 2-nm deflection results in a peak force of 200 pN. Therefore tip, sample, and force are identical in Fig. 4. Nevertheless, contact mode provides more structural information. This suggests that the applied force does not fully characterize the tip sample interaction for tapping mode. Alternatively, we suggest analyzing the energy dissipated with every touch. It is noteworthy that the tapping mode SFM was operated under conditions that were optimized for contact mode. Tapping mode might require different conditions. A systematic optimization guided by a theoretical analysis is under investigation.

Contact mode SFM has proved to be capable of atomic-scale vertical resolution on biological samples (Schabert et al., 1995). As shown above, tapping mode heights are identical to contact mode values and reveal a higher signal-to-noise ratio. Nevertheless, for all four samples the calculated standard deviation is significantly higher than atomic-scale vertical resolution. This is partially due to a small sample tilt (see Materials and Methods, data analysis).

For the rod-shaped TMV, 1 nm standard deviation of the height might correspond to flattening of the object due to the interaction with the substrate and to fluctuations of the height within different TMV rods. The expected length is 300 nm (Namba and Stubbs, 1986). The assembly of the TMV is determined by its RNA. The length of the molecules seen in Fig. 1 *b* varies. Most likely the TMV has lost its RNA, which then corresponds to a nonperfect assembly of its subunits. Deviations from the average diameter of the rod may occur.

The height variations of the tubelike polyhead are smaller than detected by any previous technique (see Table 1). Nevertheless, 10% deviation of the measured heights still requires an explanation. Flattening of the tube due to the interaction with the substrate and fluctuation of the average assembly might occur. Surprisingly, the polyheads seem to be slightly flattened on the top of the tube (see amplitude signal of Fig. 2). Because there are also hints for a weak double tip in the deflection signal the interpretation remains unclear.

The deviation of the vertical dimension of the purple membrane is the smallest. The heights are consistent between tapping and contact mode but are significantly different from literature data. The thickness of purple membranes depends on the pH of the buffer (Müller et al., 1995b). Because of the electrostatic repulsion between tip and purple membrane at common pH, low forces might cause heights that are too large.

The vertical dimension of the HPI layers matches the literature data and contact mode measurements but reveals 0.8 nm variation. Freshly cleaved HOPG is atomically flat, but high purity of all substances is needed to maintain a low background preparation. Nonspecific binding of all organic substances by hydrophobic interaction results in a high background level. Height measurements were performed while avoiding background particles, but a thin uniform layer of organic material was frequently seen (data not shown). Height profiles that were measured against the substrate were analyzed, but differentiation between the substrate and an organic contamination layer was often found to be difficult. A lower height and a reduced accuracy of the height data occur.

CONCLUSIONS

In contact mode SFM, molecules physisorbed to a flat substrate are often easily displaced by the tip because of frictional forces exerted by the tip. The use of tapping mode SFM in solution instead of contact mode greatly reduces friction and therefore enormously facilitates sample preparation. Using an oscillating fluid cell and tapping frequencies around or below 10 kHz, a vertical resolution, which is as good as in contact mode, was demonstrated. However, a similarly high lateral resolution has not yet been achieved. A better analysis of the tapping mode interaction of tip and sample is needed and is currently under investigation.

We would like to thank Peter Lusche (Berlin) for providing us with nice bunjee cords and Prof. Dr. Wolfgang Baumeister (MPI Biochemistry, Martinsried, Germany) for donations of the HPI. The purple membrane was given to us by Daniel Müller and Prof. Dr. Andreas Engel (Maurice E. Müller Institute, Biozentrum, Basel, Switzerland), who furthermore kindly provided TMV and the polyheads. Special thanks to Dr. Paul Hillner, Dr. Wolfgang Stocker, Roger Bilewicz, and Dr. Francis Wolf for reading and discussing the manuscript.

This work was supported by the ESPRIT Long Term Research Project PRONANO (8523).

REFERENCES

Amrein, M. 1989. STM on freeze-dried and Pt-Ir-C coated bacteriophage T4 polyheads. *J. Ultrastruct. Mol. Struct. Res.* 102:170–177.

Amrein, M., Z. Wang, and R. Guckenberger. 1991. Comparative study of a regular protein layer by scanning tunneling microscopy and transmission electron microscopy. *J. Vac. Sci. Technol. B.* 9:1276–1281.

Anselmetti, D., R. Lüthi, E. Meyer, T. Richmond, M. Dreier, J. E. Frommer, and H. Güntherodt. 1994. Attractive-mode imaging of biological materials with dynamic force microscopy. *Nanotechnology.* 5:87–94.

Baumeister, W., M. Barth, R. Hegerl, R. Guckenberger, R. M. Hahn, and W. O. Saxton. 1986. Three-dimensional structure of the regular surface layer (HPI layer) of *Deinococcus radiodurans*. *J. Mol. Biol.* 187: 241–253.

Bezanilla, M., B. Drake, E. Nudler, M. Kashlev, P. Hansma, and H. Hansma. 1994. Motion and enzymatic degradation of DNA in the atomic force microscope. *Biophys. J.* 67:2454–2459.

Binnig, G., C. F. Quate, and C. Gerber. 1986. Atomic force microscopy. *Phys. Rev. Lett.* 56:930–933.

Binnig, G., and H. Rohrer. 1982. Scanning tunneling microscopy. *Helv. Phys. Acta.* 55:726–735.

Butt, H.-J., K. H. Downing, and P. K. Hansma. 1990. Imaging the membrane protein bacteriorhodopsin with the atomic force microscope. *Biophys. J.* 58:1473–1480.

Butt, H. J., R. Guckenberger, and J. P. Rabe. 1992. Quantitative scanning tunneling microscopy and scanning force microscopy of organic materials. *Ultramicroscopy.* 46:375–393.

Elings, V., and J. Gurley. 1993. U.S. Patent 5,266,801.

Elings, V., and K. Kjoller. 1992. A new AFM mode for improved imaging of soft samples. *In* Workshop on STM-AFM and Standard Biological Objects. Reaumont, France.

Engel, A. 1991. Biological Applications of scanning probe microscopy. *Annu. Rev. Biophys. Biophys. Chem.* 20:79–108.

Engel, A., F. Schabert, D. Müller, and C. Henn. 1995. Imaging membrane proteins in their native environment with the atomic force microscope. *In* NATO Workshop on Scanning Probe Microscopy, and Molecular Materials. Kluwe, Schloss Ringberg, Germany.

Frommer, J., R. Lüthi, E. Meyer, D. Anselmetti, M. Dreier, R. Overney, H.-J. Güntherodt, and M. Fujihira. 1993. Adsorption at domain edges. *Nature.* 364:198.

Goldie, K. N., N. Pante, A. Engel, and U. Aebi. 1994. Exploring native nuclear pore complex structure and conformation by scanning force microscopy in physiological buffers. *J. Vac. Sci. Technol. B.* 12: 1482–1485.

Guckenberger, R., W. Wiegräbe, A. Hillebrand, T. Hartmann, Z. Wang, and W. Baumeister. 1989. Scanning tunneling microscopy of a hydrated bacterial surface protein. *Ultramicroscopy.* 31:327–332.

Hansma, H., and J. Hoh. 1994. Biomolecular imaging with the atomic force microscope. *Annu. Rev. Biophys. Biomol. Struct.* 23:115–139.

Hansma, P. K., et al. 1994. Tapping mode atomic force microscopy in liquids. *Appl. Phys. Lett.* 64:1738–1740.

Hegner, M., P. Wagner, and G. Semenza. 1993. Immobilizing DNA on gold via thiol modification for atomic force microscopy imaging in buffer solutions. *FEBS Lett.* 336:452–456.

Hoh, J. H., R. Lal, S. A. John, J.-P. Revel, and M. F. Arnsdorf. 1991. Atomic force microscopy and dissection of gap junctions. *Science.* 253:1405–1408.

Karrasch, S., M. Dolder, F. Schabert, J. Ramsden, and A. Engel. 1993. Covalent binding of biological samples to solid supports for scanning probe microscopy in buffer solution. *Biophys. J.* 65:2437–2446.

Karrasch, S., R. Hegerl, J. H. Hoh, W. Baumeister, and A. Engel. 1994. Atomic force microscopy produces faithful high-resolution images of protein surfaces in an aqueous environment. *Proc. Natl. Acad. Sci. USA.* 91:836–838.

Müller, D. J., G. Büldt, and A. Engel. 1995a. Force-induced conformational change of bacteriorhodopsin. *J. Mol. Biol.* 249:239–243.

Müller, D., F. Schabert, G. Büldt, and A. Engel. 1995b. Imaging purple membranes in aqueous solution at sub-nanometer resolution by atomic force microscopy. *Biophys. J.* 68:1681–1686.

Namba, K., and G. Stubbs. 1986. Structure of tobacco mosaic virus at 3.6 Å resolution: implications for assembly. *Science.* 231:1401–1406.

Oesterheld, D., and W. Stoeckenius. 1974. Isolation of the cell membrane of *Halobacterium halobium* and its fractionating into red and purple membrane. *Methods Enzymol.* 31:667–678.

Ohnesorge, F., and G. Binnig. 1993. True atomic resolution by atomic force microscopy through repulsive and attractive forces. *Science.* 260: 1451–1456.

Putman, C. A. J. 1994. Development of an atomic force microscope for biological applications. University of Twente.

Putman, C. A. J., K. O. van der Werft, B. G. de Grooth, N. F. van Hulst, J. Greve, and P. K. Hansma. 1992. A new imaging mode in the atomic force microscopy based on the error signal. *SPIE.* 1639:198–204.

Radmacher, M., M. Fritz, H. G. Hansma, and P. K. Hansma. 1994. Direct observation of enzyme activity with the atomic force microscope. *Science.* 265:1577–1579.

Schabert, F., and A. Engel. 1994. Reproducible acquisition of *E. coli* porin surface topographs by atomic force microscopy. *Biophys. J.* 67: 2394–2403.

Schabert, F., and A. Engel. 1995. Atomic force microscopy of biological membranes: current possibilities, and prospects. *In* NATO ASI series E: Applied Sciences. Kluwer Academic Publishers, Schluchsee, Germany.

Schabert, F., A. Hefti, K. Goldie, A. Stemmer, A. Engel, E. Meyer, R. Overney, and H. J. Guntherodt. 1992. Ambient-pressure scanning probe microscopy of 2D regular protein arrays. *Ultramicroscopy.* 42: 1118–1124.

Schabert, F., C. Henn, and A. Engel. 1995. Native *Escherichia coli* OmpF porin surfaces probed by atomic force microscopy. *Science.* 268:92–94.

Schabert, F. A., J. H. Hoh, S. Karrasch, A. Hefti, and A. Engel. 1994a. Scanning force microscopy of *E. coli* OmpF porin in buffer solution. *J. Vac. Sci. Technol. B.* 12:1504–1507.

Schabert, F., H. Knapp, S. Karrasch, R. Haring, and A. Engel. 1994b. Confocal scanning laser–scanning probe hybrid microscope for biological applications. *Ultramicroscopy.* 53:147–157.

Shao, Z., and J. Yang. 1995. Progress in high resolution atomic force microscopy. *Q. Rev. Biophys.* 28:195–251.

Stemmer, A., and A. Engel. 1990. Imaging biological macromolecules by STM: quantitative interpretation of topographs. *Ultramicroscopy.* 34: 129–140.

Steven, A. C., E. Couture, U. Aebi, and M. K. Showe. 1976. Structure of T4 polyheads. *J. Mol. Biol.* 106:187.

Unwin, P. N. T., and A. Klug. 1974. Electron microscopy of the aggregate of tobacco mosaic virus protein. I. Three-dimensional image reconstruction. *J. Mol. Biol.* 87:641–656.

Vesenka, J., S. Manne, R. Giberson, T. Marsh, and E. Henderson. 1993. Colloidal gold particles as an incompressible atomic force microscope imaging standard for assessing the compressibility of biomolecules. *Biophys. J.* 65:992–997.

Wang, Z., T. Hartmann, W. Baumeister, and R. Guckenberger. 1990. Thickness determination of biological samples with a z-calibrated scanning tunneling microscope. *Proc. Natl. Acad. Sci. USA.* 87:9343–9347.

Wiegräbe, W., M. Nonnenmacher, R. Guckenberger, and O. Wolter. 1991. Atomic force microscopy of a hydrated bacterial surface protein. *J. Microsc.* 163:79–84.

Wildhaber, I., H. Gross, A. Engel, and W. Baumeister. 1985. The effect of air-drying and freeze-drying on the structure of a regular protein layer. *Ultramicroscopy.* 16:411–422.

Yang, J., L. K. Tamm, T. W. Tillack, and Z. Shao. 1993. New approach for atomic force microscopy of membrane proteins—the imaging of cholera toxin. *J. Mol. Biol.* 229:286–290.

Zenhausern, F., M. Adrian, R. Emch, M. Taborelli, M. Jobin, and P. Descouts. 1992. Scanning force microscopy and cryo-electron microscopy of tobacco mosaic virus as a test specimen. *Ultramicroscopy.* 42:1168–1172.